ARTICLES

Controlled Confinement and Release of Gases in Single-Walled Carbon Nanotube Bundles

Christopher Matranga* and Bradley Bockrath

National Energy Technology Laboratory, United States Department of Energy, P.O. Box 10940, Pittsburgh, Pennsylvania 15236-0940

Received: December 14, 2004; In Final Form: March 11, 2005

A simple procedure is described that locks small quantities of SF_6, CO_2, and $^{13}CO_2$ into opened single-walled carbon nanotube (SWNT) bundles and keeps the gas in the SWNTs above the desorption temperature of these molecules. The technique involves opening the SWNTs with ozonolysis at 300 K followed by vacuum-annealing at 700 K. Gases are then cryogenically adsorbed into the opened SWNTs and locked into the SWNT pores by functionalizing the sample with a low-temperature ozone treatment. The low-temperature ozone treatment functionalizes the entry ports into the SWNT pores, which in turn create a physical barrier for gases trying to desorb through these functionalized ports. The samples are stable under vacuum for periods of at least 24 h, and the trapped gases can be released by vacuum-heating to 700 K. Reduced quantities of the trapped gases remain in the SWNTs even after exposure to room air. Fourier transform infrared spectroscopy is used to monitor the functionalities resulting from the ozone treatment and to detect the trapped gas species.

Introduction

In this report, we describe a relatively straightforward procedure for placing small quantities of gas-phase SF_6, CO_2, and $^{13}CO_2$ into single-walled carbon nanotube (SWNT) bundles and keeping these gases locked within the bundles above the desorption temperature of these molecules. This report shows that the physical trapping of a variety of gases in a SWNT bundle is a viable technique warranting further development.

New methodologies for controlling the confinement and release of molecules in the hollow pores of SWNT bundles should be of broad interest. From a scientific standpoint, the endohedral and interstitial spaces of a SWNT bundle provide an environment to study a variety of properties associated with low-dimensional molecular systems. One can even envision loading these spaces with different molecules and attempting reaction chemistry inside of the pores[1] of a SWNT bundle.

From a technological perspective, SWNTs are being evaluated as novel electronic devices[2,3] and sensors.[4−6] The properties of these of devices should be dependent on the types of impurities present within the bundle. The ability to control this impurity by locking the dopant inside of the bundle would be highly advantageous. It has even been suggested that the locking of gases such as ^{133}Xe into low-dimensional pores could be useful in imaging applications.[7]

The encapsulation of C_{60} and organic molecules in SWNT bundles has been achieved by heating SWNT samples with these species and allowing for thermal diffusion to load the pores of the bundle.[8−11] Since the species is not physically locked inside of these pores, subsequent heating should cause the encapsulated species to be ejected from the SWNT bundle at some temperature comparable to the physisorption energy in its adsorption site. It is therefore desirable to develop techniques that will allow one to lock species inside the SWNT pores at temperatures above this desorption temperature.

More permanent methods for encapsulation have also been reported. For multiwalled carbon nanotubes (MWNTs), Ar encapsulation was achieved by isostatically pressing MWNT samples at 650 °C and 170 MPa for 48 h.[7] The trapped Ar was detected with energy-dispersive X-ray spectroscopy (EDS) and shown to be inside the tubes with X-ray intensity maps of the trapped Ar gas. Even though this technique is rather effective, the extreme pressure conditions necessary to trap gases motivates us to explore other possibilities.

Techniques for trapping have been reported that do not require the extreme pressure conditions reported for MWNT systems. In this regard, the trapping of CO_2 inside the endohedral and interstitial spaces of SWNT bundles was found to occur.[12,13] Trapping was accomplished by functionalizing the sample with an acid treatment followed by vacuum-annealing at 700 K. The annealing step causes a partial thermolysis of the functional groups on this sample that are believed to generate CO_2.[12,13] Steric rearrangements of the remaining functionalities associated with CO_2 generation are thought to physically block the gas from exiting the SWNT pores. The trapped CO_2 generated in this manner is found to be stable for periods of months, survives temperature cycling in a vacuum from 5 to 700 K, and is even present after venting the samples to room air. Since this type of trapping seems to be the fortuitous result of how these acid-created functionalities decompose and simultaneously lock the gas in place, it is not obvious that other trapped gases can be produced with different functionalization schemes.

In this paper, we report a simple technique for the controlled confinement and release of gases inside of SWNT bundles using commercially available equipment. Our motivation is to develop new trapping techniques that will be applicable to a broad range

* Author to whom correspondence should be addressed. E-mail: matranga@netl.doe.gov.

10.1021/jp044307m
Published on Web 04/09/2005

of gas species. The current work differs significantly from previous efforts reported[12,13] from our research group because we are now able to display a certain degree of control over which molecules we trap in our SWNT samples. We illustrate this control by trapping SF_6, CO_2, and $^{13}CO_2$ into our SWNT samples. We are then able to cycle the samples in a vacuum between 77 and 300 K over 24−72 h without releasing the trapped gas. Ultimately, the release of the trapped gas is achieved by vacuum-heating to 700 K. Our ability to control the confinement of light gases in SWNT bundles represents progress in developing new techniques for fabricating low-dimensional molecular systems.

Experimental Section

Samples made by the HiPco process were obtained as unpurified solid material from Carbon Nanotechnologies Incorporated and are reported to have sample purities of SWNT carbon that are greater than 90 atomic %.[14] From thermogravimetric analysis (TGA), we find that this material has ∼18 wt % (mass Fe/mass of sample) of residual Fe catalyst in agreement with previous reports.[14] The unpurified HiPco nanotubes were later dispersed in toluene so thin films could be made for IR analysis.

Fourier transform infrared (FTIR) studies were done in the transmission geometry with the samples housed in a stainless steel vacuum chamber described previously.[13] Infrared samples were thin films prepared by dispersing the sample directly on a plane parallel CaF_2 window (Janos Technology) and evaporating the solvent in a 120 °C oven for ∼5 min.[12,13,15] The thickness of the film was adjusted to give a background optical density (OD) of ∼1.1−1.3 at 2300 cm^{-1}, which gave enough sample thickness for us to observe the small quantities of trapped gases seen in this study.

Ozone-etching of the sample is conducted with a Pacific Ozone Technology L21 model ozone generator (corona arc discharge method) using an oxygen gas source, a reactor pressure of ∼10 pounds per square inch, and a flow rate of ∼10 standard cubic feet per hour. Under these conditions, this system produces a mixed ozone/oxygen gas stream that is ∼4 wt % in ozone. Ozone delivery into the infrared cell was verified by infrared observation of the ozone band at 1043 cm^{-1}.[16] We are able to observe this band for the entire dosing period when ozonizing the SWNT samples (∼10 min). This indicates that the sample is always in contact with ozone during dosing and that ozone decomposition in the cell is not a significant issue for these short dosing periods.

The SWNT samples are placed into the vacuum chamber and pumped down for ∼48 h, yielding a base pressure of ∼2 × 10^{-8} Torr. The sample is then etched for 10 min at 300 K with 10 Torr ($P_{ozone} + P_{oxygen}$) of the ozone/oxygen mixture, vented to the vacuum-pumping system for ∼20−30 min, yielding a pressure of ∼5 × 10^{-7} Torr, and then vacuum-annealed at 700 K for 2−3 h. This etching/heating procedure is completed two times. As reported previously, this type of etching/heating procedure is believed to open up access to the endohedral sites of the SWNT bundles.[1,17−20]

After the etching/heating procedure is carried out twice, the sample is vacuum-pumped overnight, yielding a base pressure of ∼2 × 10^{-8} Torr. The sample is cooled to 175 K, and the cell is charged with SF_6 (∼12 mTorr), CO_2 (∼1.0 Torr), or $^{13}CO_2$ (∼1.0 Torr) to physisorb these species into the SWNT bundle. Infrared spectra are then collected of the physisorbed species. The chamber is then backfilled with the ozone/oxygen mixture until the total pressure of the chamber is ∼10 Torr, and the sample is left in this environment for 10 min. The sample is then vented to the vacuum-pumping system and heated to 300 K for 3−4 h before any further infrared studies are conducted. A temperature of 175 K was chosen for physisorption and trapping because it is slightly above the boiling point of ozone (161.3 K), thus reducing the amount of ozone adsorption occurring on the cooling Dewar and sample holder.

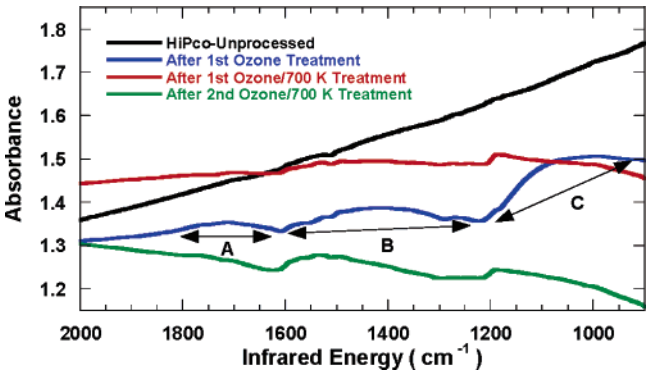

Figure 1. Infrared spectra of the SWNT samples at 300 K. These spectra are raw absorbance data and have not been processed to account for sloping baselines occurring because of the optical properties of the SWNT film.

Ex situ Raman measurements were done with a dispersive Nicolet Almega spectrometer at ∼2 cm^{-1} resolution over the spectral range presented. Approximately 15 mW of the 150 mW laser source (532 nm) was focused on the sample with a 10× microscope objective, and the Raman signal was detected in the backscattering geometry. Measurements were done directly on the samples used in the infrared experiments while still dispersed on the CaF_2 window mentioned above.

Results and Discussion

To fully open up the SWNT bundles for gas adsorption in the endohedral sites, we first use an ozone-etching procedure. It has been shown previously that ozone treatment followed by vacuum-annealing enhances access to the endohedral sites of SWNT bundles.[1,17−20] Facile endohedral access will be needed to successfully lock molecules into these pores. For trapping experiments with large molecules such as SF_6, this etching procedure was necessary to get any evidence of adsorption and trapping inside of the SWNT bundle. In experiments on CO_2, endohedral adsorption and trapping could be achieved in the unprocessed HiPco sample (not etched) and also after etching this sample with ozone. For simplicity, we only report on trapping in samples that have been ozone-etched prior to adsorption/trapping experiments.

Typical infrared results for the sample during an etching/heating cycle are displayed in Figure 1. For clarity, we have not subtracted out any of the sloping background absorption due to electronic absorptions of the SWNT film in the midinfrared[21] and instead present unprocessed absorbance data. Initially, the unprocessed HiPco sample shows little evidence of oxygen-containing functionalities. Treatment with the ozone/oxygen mixture produces three broad features in the spectra between (A) 1600 and 1800 cm^{-1}, (B) 1200 and 1600 cm^{-1}, and (C) 900 and 1200 cm^{-1}. The regions labeled A, B, and C are, respectively, where carbonyl, C═C vibrations and C−O vibrations are expected to occur on nanostructured carbons.[19,20,22,23] Vacuum-annealing at 700 K softens these features, flattens the broadband optical background of the film, and leaves a fairly prominent peak at ∼1180 cm^{-1}. The feature at 1180 cm^{-1} is consistent with a C−O-type vibration. C−O bonds from

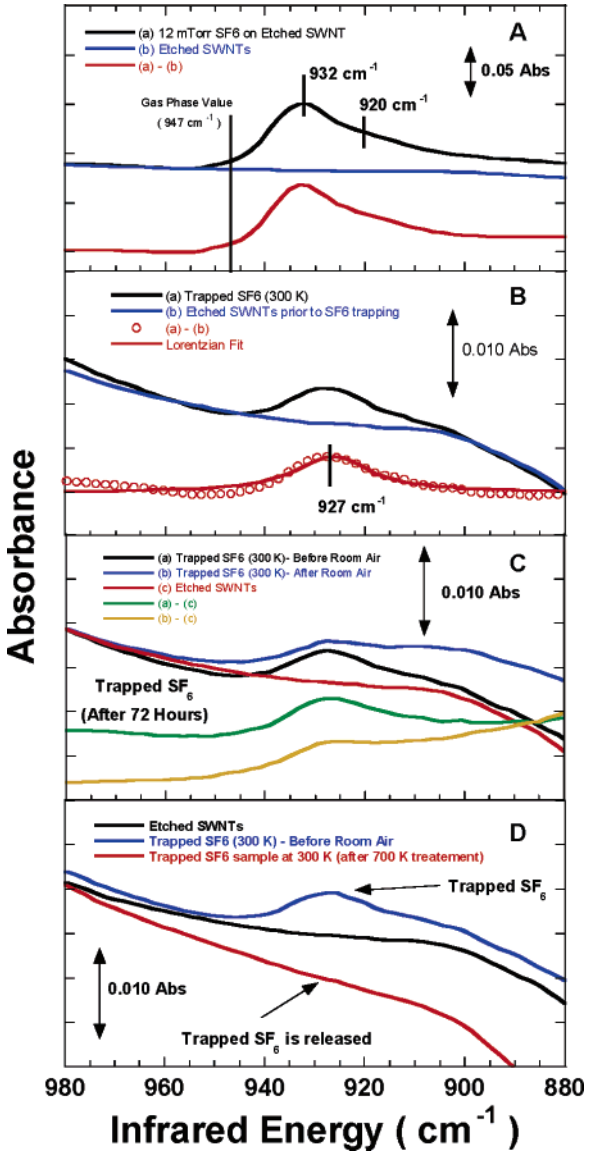

Figure 2. Infrared spectra of physisorbed and trapped SF_6. (A) Physisorption of SF_6 at 12 mTorr and 175 K. The raw absorbance data (black line), SWNTs prior to SF_6 dosing (blue line), and the difference between the two (red line). (B) Trapped SF_6 after 24 h of vacuum-pumping. (C) Trapped SF_6 after 72 h (black line) and after venting to room air (blue line). (D) Trapped SF_6 before and after the vacuum-heating step.

ozonides and other types of functionalities have been seen in both experimental and computational studies conducted on the ozone oxidation of SWNTs.[19,20,24−26] A second etching/heating cycle does not create any new features and only serves to decrease the overall optical density of the film by ∼15%. After the second etching/heating cycle, we typically see less flattening of the optical features in this region in comparison to the first cycle.

Results for SF_6 adsorption on the etched/heated sample at 12 mTorr and 175 K are shown in Figure 2A. SF_6 adsorption on the etched/heated SWNT sample results in a strong infrared band at 932 cm^{-1} with a lower-energy shoulder at 920 cm^{-1}. These vibrations are shifted from the 947 cm^{-1} value[27] for the υ_3 band of gas-phase SF_6 by 15 and 27 cm^{-1}, respectively. The red-shifting of the 932 and 920 cm^{-1} peaks from the gas-phase peak is typical of molecules physisorbed inside the endohedral pores of SWNT bundles[1,12,13,15,17,18] and indicates that SF_6 interacts strongly with the SWNT sample.

If the features seen in Figure 2A arise from endohedral or interstitial adsorption, then we expect that functionalization of the SF_6-dosed sample might lock the physisorbed gas into these pores. Functionalites are known to block the entrance of gases into the endohedral and interstitial pores of SWNT bundles. This occurs because these bulky functional groups decorate the structural defects that allow access to these adsorption sites and act as physical barriers to adsorption.[1,17−19,28] On the basis of this, it is rather intuitive to preload these adsorption sites with a gas and to try to lock the gas in place by functionalizing the exit ports from these pores. In essence, instead of using functional groups to block access to adsorption sites, we will be using them to keep molecules inside of these sites.

To test this idea, we adsorb SF_6 on the sample at 12 mTorr and 175 K as illustrated in Figure 2A. After the SF_6 adsorption was confirmed with infrared spectroscopy, the infrared cell is backfilled with the ozone/oxygen mixture up to 10 Torr for 10 min to functionalize the sample and lock the SF_6 into the bundle. We then vent the sample to vacuum and heat it to 300 K. After leaving the sample to degas under vacuum-pumping at 300 K overnight, we find infrared evidence that SF_6 is still trapped in the sample (Figure 2B). This evidence is seen as a single infrared peak at 927 cm^{-1}, which has a full width at half-maximum (fwhm) of ∼19 cm^{-1} as determined from a Lorentzian fit to the data (red line, Figure 2B). This peak is close in energy to the band seen at 932 cm^{-1} for physisorbed SF_6, suggesting that a similar SWNT site is responsible for both peaks. Cooling the sample to 77 K and reheating to 300 K does not create any changes in this infrared peak.

Subsequent cooling/heating cycles (three total) between 77 and 300 K over the next 2 days does little to change the band at 927 cm^{-1}. After approximately 72 h, the band at 927 cm^{-1} is still present (black line, Figure 2 C). This indicates that the sample is stable when kept under vacuum.

To test if the sample is stable under ambient conditions, we vent the sample to room air, collect ex situ Raman spectra (see below), and return the sample to the vacuum chamber. We then check for trapped SF_6 after a 48 h pump down. After the venting and 48 h pump down steps, we still see the trapped SF_6 band at 927 cm^{-1} (blue line, Figure 2C), although the intensity of the band relative to the baseline appears to be lower, indicating that some of the trapped gas may have been released. The loss of intensity implies that the blocking functionalities are sensitive to room air exposure. Moisture in the air could cause the hydrolysis of any ozonides or other labile functional groups responsible for locking the SF_6 into the bundles. Modification of SWNT functionalities around structural defects by the oxygen present in room air could also be responsible. The changes to the infrared spectra in the region from 2000 to 1000 cm^{-1} during exposure to room air are subtle, resulting only in slight baseline changes (see below). This suggests that any functionality changes that are occurring are minor and below our detection limits.

This shifting of the background absorption features of the film after exposure to room air can be seen clearly in Figure 2C. This is seen in the baseline shift between 900 and 960 cm^{-1} of the trapped SF_6 sample after exposure to room air (blue line, Figure 2C). Baseline shifting is also seen in Figure 1 where functionalization and defunctionalization can cause changes in the overall slope associated with the baseline features of the SWNT film. We suspect this baseline shifting is, at least in part, related to how functionalization perturbs the broadband optical properties of these films in the midinfrared.[21]

Since functionalization seems to be responsible for locking the SF_6 within the bundle, one might expect that the complete

or partial removal of functionalities might release the trapped species. It has previously been shown that vacuum-heating is effective in removing functionalities from SWNT samples.[19,23,28,29] The changes that vacuum-heating to 700 K has on the functional groups present on the ozone-treated samples were shown earlier in Figure 1.

To test this idea, we vacuum-heat the sample to 700 K for ~5 h after it was exposed to room air. The sample is then cooled to 300 K. After this treatment, we can see that the peak at 927 cm^{-1} is absent from the infrared spectra, indicating that the trapped SF_6 was released. Cooling to 77 K does not change the infrared spectra of Figure 2D.

To show that this trapping procedure can be extended to other chemical systems, we have also trapped CO_2 in SWNT bundles. Infrared spectra for adsorbed CO_2 in the ozone-etched SWNTs at 175 K and 1.0 Torr are shown in Figure 3A. Adsorption of CO_2 results in a large infrared feature at 2330 cm^{-1} that is shifted from the gas-phase value of 2349 cm^{-1} for the υ_3 asymmetric stretching mode by 19 cm^{-1}. Previous experimental and computational studies have assigned the feature at 2330 cm^{-1} to endohedrally adsorbed CO_2.[12,13,15,18] Another smaller shoulder is seen at 2315 cm^{-1} in Figure 3A. This feature is seen in the raw absorbance spectra and therefore is not an artifact caused by subtracting the etched SWNT contribution from the background. The feature at 2315 cm^{-1} has not been reported in previous work.[12,13,15,18] It is not seen until after the samples are etched, indicating that access to this site is opened by the ozone-etching procedure. This type of behavior would be consistent with adsorption in an endohedral site.

For trapping, we predose the sample with CO_2 to 1.0 Torr as shown in Figure 3A. We then backfill the chamber with the ozone/oxygen mixture until the total pressure in the cell is 10 Torr. After 10 min in this atmosphere, we vent the sample to the vacuum-pumping system and heat it to 300 K. After 3 h at 300 K, the cell pressure is $\sim 3 \times 10^{-8}$ Torr. We then use infrared spectroscopy to probe for trapped CO_2.

In the infrared spectra, we see trapped CO_2 as shown by a peak at ~2330 cm^{-1}. This peak is visible in the raw absorbance spectra (Figure 3B) and is not an artifact introduced from subtracting the background contribution of the SWNT film. The shifting slope of the background after trapping the CO_2 is evident when comparing the infrared spectra for the etched SWNT sample prior to trapping (black line, Figure 3B) to that seen for the samples with the trapped CO_2. This shifting is likely a result of changes that the ozone functionalization step causes in the broadband optical properties of this film. To subtract out this background, we simply fit the sloping background of each infrared spectra to a polynomial expression excluding the CO_2 resonance region from ~2280−2370 cm^{-1}. This sloping background is then subtracted from each individual spectrum. The results of this background subtraction are shown in Figure 3C.

In Figure 3C, the peak at ~2330 cm^{-1} is evident. This peak is nearly identical in energy to the 2330 cm^{-1} seen in Figure 3A and suggests it is attributable to a similar site in the SWNT bundle. As mentioned above, a feature at ~2330 cm^{-1} has been associated with endohedrally physisorbed and trapped CO_2 molecules.[12,13,15,18] We therefore attribute the feature in Figure 3C to endohedrally trapped CO_2.

Figure 3C also shows that the intensity of this peak varies with temperature. This phenomenon was noted in previous work[12,13] on trapped CO_2 although the mechanism for it is not understood. Lorenztian fits to the spectra in Figure 3C show that the intensity ratio of the trapped CO_2 features at 77 and 300 K is ~4, which is comparable to the ratio of ~2−3 noted in previous work.[12, 13]

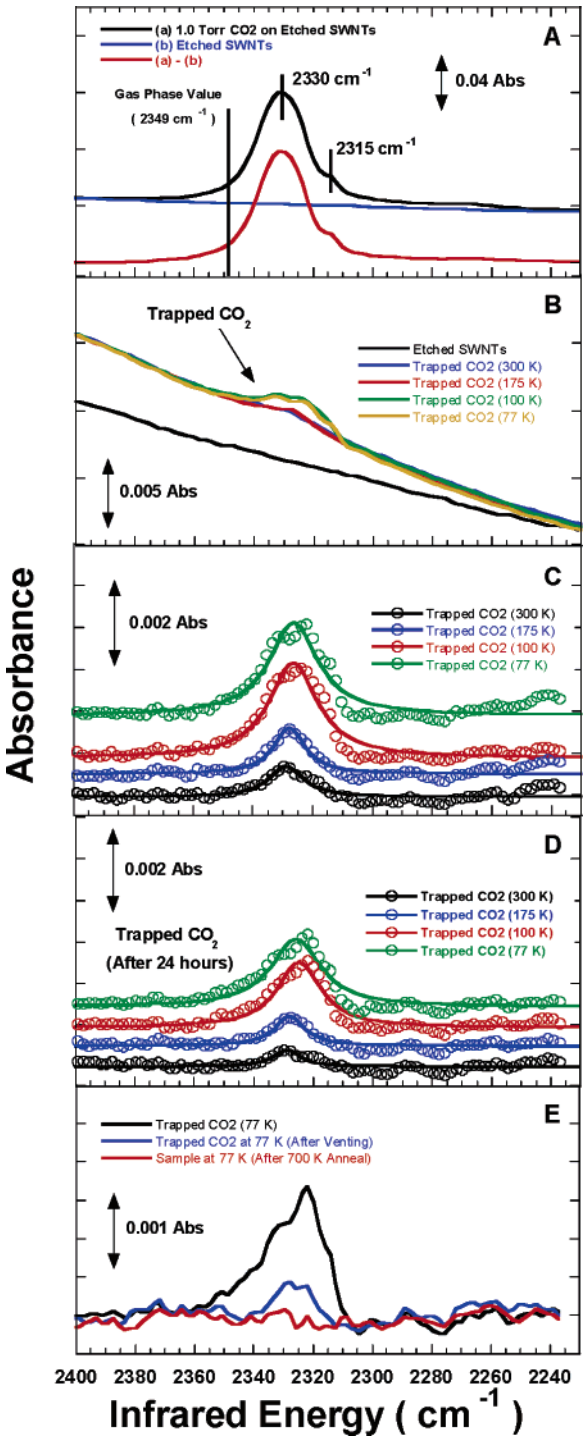

Figure 3. Infrared spectra for physisorbed and trapped CO_2. (A) Physisorption at 1.0 Torr and 175 K. (B) Raw absorbance data for trapped CO_2 illustrating that the 2330 cm^{-1} peak is visible in the unprocessed spectra. (C) Data for trapped CO_2 after the background/baseline subtraction procedure described in the text. Open circles are experimental data, and solid lines are Lorentzian fits. (D) Trapped CO_2 after 24 h of vacuum-pumping. Open circles are experimental data, and solid lines are Lorentzian fits. (E) Trapped CO_2 before (black line) and after (blue line) room air exposure. Vacuum-annealing to 700 K removes any evidence of trapped CO_2.

It is useful to compare the quantities of trapped CO_2 seen in the current study to previous reports.[12,13] To make a rough comparison, we compare the integrated intensities of the ~2330

cm^{-1} band at 77 K in Figure 3C to the integrated intensities for trapped CO_2 in our previous work. This relies on assuming that the infrared cross section for the υ_3 band is not overly sensitive to its adsorption environment. Direct comparison of the integrated intensities shows that the band in Figure 3C is about as intense as the trapped CO_2 reported in HNO_3-treated HiPco samples.[12] Comparing Figure 3C to the integrated intensity of the 2330 cm^{-1} band in acid-purified nanotubes synthesized by laser ablation shows that the feature in Figure 3C is approximately 7 times lower in intensity.[13] The OD of the SWNT films in previous work[12,13] was ~1.0 at 2330 cm^{-1} and in the current work is 1.1−1.3. Assuming that the optical density is linear with the SWNT film thickness, then these intensity comparisons for trapped CO_2 should be good to within ~10−30%. Overall, these comparisons show that the trapping of CO_2 by the procedure described in this study is reasonably effective when compared to the amounts of encapsulated CO_2 produced by previously reported techniques.[12,13]

After the sample was vacuum-pumped at 300 K for 24 h, the peak attributed to trapped CO_2 is still present (Figure 3D). The intensity variations with temperature seen above are also noted. The data in Figure 3D indicate that this sample is stable under vacuum for periods of at least 24 h.

In contrast, venting the trapped CO_2 sample to room air and returning it to the vacuum chamber results in a significant loss of intensity to the peak at ~2330 cm^{-1}. The intensity of this peak is too low to be seen at 300 K, and it is only after cooling the sample to 77 K that the band starts to become visible (Figure 3E). This cooling step takes advantage of the temperature-dependent intensity noted for the trapped CO_2 species and therefore can make a band that is within the experimental noise at room temperature detectable at low temperatures. As seen for the case of SF_6, vacuum-heating of the sample to 700 K completely removes any infrared evidence of trapped CO_2 (Figure 3E).

The larger relative intensity change seen for CO_2 after venting in comparison to SF_6 could be related to the size of the molecules. If changes in the functionalities around structural defects during room air exposure are releasing the trapped molecules, then larger molecules, such as SF_6, would have more difficulty getting past these physical barriers.

Since our trapping procedure involves an oxidative ozone treatment, one might argue that the trapped CO_2 seen in Figure 3 actually originated from the oxidation of the SWNT carbon and was not a result of locking the physisorbed CO_2 into the bundle. To test this, we have performed trapping experiments using $^{13}CO_2$ (~99% ^{13}C, Cambridge Isotope Laboratories).

Adsorption of $^{13}CO_2$ is shown in Figure 4A. A prominent peak is seen at 2267 cm^{-1} with a smaller shoulder at 2250 cm^{-1}. These features are shifted from the gas-phase value of 2284 cm^{-1} for the υ_3 mode of $^{13}CO_2$ by 17 and 34 cm^{-1}, respectively. This red-shifting is nearly identical in magnitude to what was seen during the physisorption of CO_2 as displayed in Figure 3A. We note that there is a small amount of CO_2 impurity in the $^{13}CO_2$ source as illustrated by the inset of Figure 4A. We therefore expect the possibility of seeing trapped CO_2 in these experiments in addition to trapped $^{13}CO_2$.

When the trapping experiment is conducted as described earlier, we see an infrared peak for trapped $^{13}CO_2$ at ~2261 cm^{-1} (Figure 4B). The intensity of the trapped $^{13}CO_2$ peak at ~2261 cm^{-1} appears to vary with temperature just as was noted above for the CO_2 band at 2330 cm^{-1}. The intensity ratio of the ~2260 cm^{-1} peak at 77 and 300 K is ~2 and comparable to previous reports for trapped CO_2.[12,13]

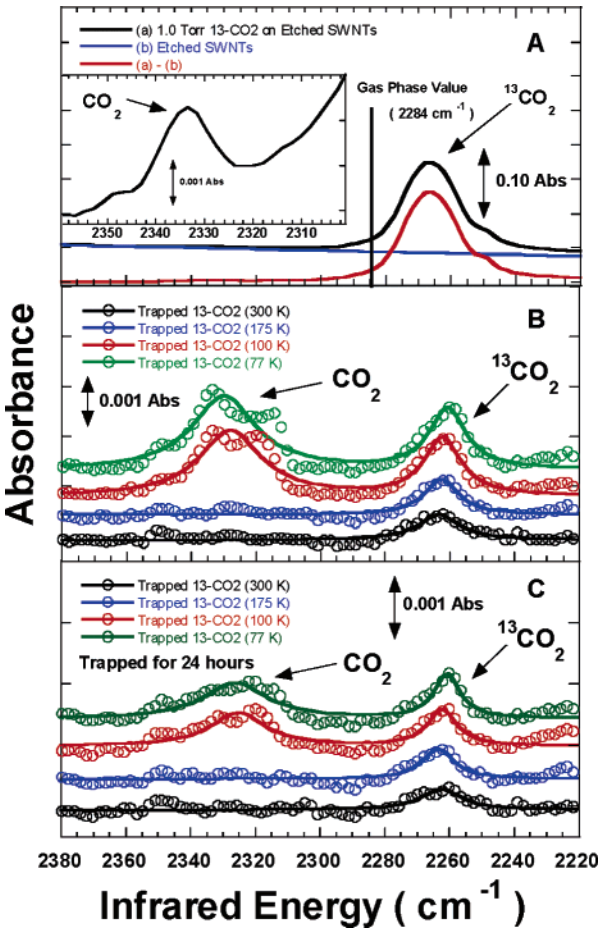

Figure 4. Infrared spectra for physisorbed and trapped $^{13}CO_2$. (A) Physisorbed $^{13}CO_2$ at 1.0 Torr and 175 K. (B) Trapped $^{13}CO_2$ and the trapped CO_2 created from ^{12}C present in the $^{13}CO_2$ source. Open circles are baseline-subtracted data points (see text), and solid lines are a fit to a single (300 and 175 K) or double (100 and 77 K) Lorentzian line shape. (C) Trapped $^{13}CO_2$ sample after 24 h of vacuum-pumping.

As the sample is cooled to 100 and 77 K, we also see evidence for trapped CO_2 in the spectra of Figure 4B as shown by the appearance of a peak at ~2330 cm^{-1}. We suspect that the small quantities of CO_2 present in the $^{13}CO_2$ gas source are responsible for this trapped CO_2. The increased intensity of the CO_2 band at low temperatures (see above) makes the band easier to detect at these temperatures. To show that this peak at ~2330 cm^{-1} does not arise from adsorption of background gases in the vacuum chamber, we hold the trapped $^{13}CO_2$ sample at 77 K for 12 h and monitor the infrared spectra while vacuum-pumping. The background pressures during this experiment are typically $\sim 5 \times 10^{-9}$ Torr and are lower than the ambient background pressure when the sample is at 300 K ($\sim 2 \times 10^{-8}$ Torr). This lowered pressure is a result of the cryopumping effect that the cold sample holder and cooling Dewar have. The intensity of the peak at 2330 cm^{-1} does not increase during this experiment as one would expect for the adsorption of background gases on the SWNT sample due to this cryopumping effect. This shows conclusively that the CO_2 peak at 2330 cm^{-1} in Figure 4B arises from trapped CO_2 within the sample and not from physisorbed ambient gas.

The trapped $^{13}CO_2$ in the sample is still present after 24 h of vacuum-pumping with the sample at 300 K (Figure 4C). Heating the sample to 700 K causes the disappearance of the peaks associated with the trapped $^{13}CO_2$ and CO_2 species (not shown). After it was heated to 700 K, cooling the sample to 77 K does not make the bands associated with the trapped $^{13}CO_2$ detectable

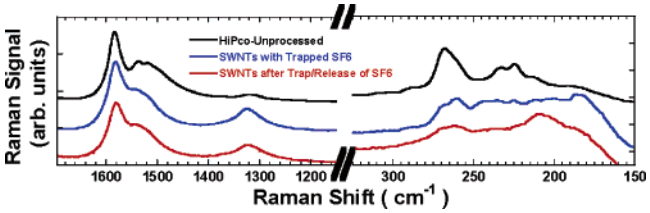

Figure 5. Representative Raman spectra of the SWNT samples from this study.

with infrared spectroscopy. This indicates that all of the detectable trapped $^{13}CO_2$ has been released from the SWNT bundle. All of the results for $^{13}CO_2$ are analogous to those found with CO_2 and confirm that the origin of the trapped species is physisorbed gas that we lock into the bundles with the ozone treatment.

As a control experiment, we have physisorbed both SF_6 at 12 mTorr and CO_2 at 1.0 Torr in separate experiments onto the ozone-etched/vacuum-annealed samples at 175 K. The physisorbed SF_6 and CO_2 produce the infrared features noted in Figures 2A and 3A, respectively. We then heat the samples to 300 K while vacuum-pumping. In both experiments, the SF_6 and CO_2 completely desorb from the sample during heating, and we see absolutely no infrared evidence for either at 300 K. Recooling the sample to 77 K does not cause the appearance of bands for either species. This control experiment illustrates that neither gas can be physisorbed in the SWNT bundle at 300 K while we vacuum-pump on the sample. It also conclusively shows that the ozone treatment used after gas physisorption is responsible for locking the gas into the SWNT. This result shows that the trapping technique described here truly does lock gases into the SWNT bundles at temperatures above their desorption points.

To prove that the ozone treatments used in this work do not significantly disrupt our SWNTs, we perform Raman spectroscopy on the samples used in the trapping experiments. Ex situ Raman is done on the samples prior to the experiments, when the samples with the trapped gas are vented to room air, and after the trapped gases are released with the 700 K heating step. These spectra are taken directly on the SWNT thin films used in the adsorption and trapping experiments.

Representative Raman spectra are shown in Figure 5 from one of the SF_6 studies. The results are typical of all samples reported here. In Figure 5, the radial breathing modes (RBMs) seem to be effected by the steps taken to trap molecules in the bundle. The relative intensity of the RBMs at 265 cm^{-1} and those from 210 to 240 cm^{-1} decrease after ozone treatment and trapping. A similar loss of RBM intensity for smaller nanotubes was noted after solution-phase ozonolysis and was seen for a variety of laser excitation frequencies.[30] This result was attributed to a diminished Raman signal from smaller tubes because functionalization can decrease the scattering cross section from these species.[30]

The ozone-etching and trapping steps seem to cause an intensity increase for the D-band of the sample at ~1330 cm^{-1}. This intensity increase is indicative of an increased density of defects in the sp^2 hybridized network of SWNT carbon. This is consistent with the functionalization indicated in Figure 1 and with the etching of defect sites in the sample.[30−32] A similar D-band intensity increase was noted in previous ozonolysis studies.[30−32]

Overall, the results in Figure 5 show conclusively that the unique electronic and vibrational properties of the SWNTs are intact as shown by the RBMs and G-bands seen. These features are present through the entire trapping and release procedure and are only slightly modified from this process. This would indicate that the trapped molecules are locked in the pores of the SWNT bundle and not in some other form of carbon created during the ozone oxidation procedure.

We point out that it should be possible to trap other gases and vapors with the technique reported here. We focused on CO_2 and SF_6 because they both have vibrations with large infrared intensities, making them easy to detect with FTIR. Also, the binding energy for these molecules in the endohedral spaces is expected to be relatively strong, making it less likely that these gases will desorb during the trapping step. The zero-coverage endohedral binding energies are estimated to be ~170−220 meV for CO_2[15,18,33]and ~320 meV for SF_6.[34] For higher coverages of CO_2, the average potential energy of endohedrally bound CO_2 increases to ~318 meV because of adsorbate−adsorbate interactions.[15]

One obvious candidate to consider for future trapping experiments would be Xe. Xe has an endohedral adsorption energy of ~220−280 meV,[29,34,35] which is comparable to CO_2 and SF_6. Xe is also known to displace CO_2 from SWNT bundles, further indicating that it has a competitive interaction with the bundle.[15,18] Since Xe is clearly not infrared-active, it is impossible for us to study it with our current experimental setup.

Weakly bound gases will likely be more problematic for trapping. Attempts at trapping CO and CH_4 at 175 K were understandably unsuccessful because we were unable to detect any gas physisorption with FTIR at the pressures accessible in our experiment. Adsorption of CF_4 in our samples at 175 K does produce the infrared signatures previously attributed to endoheral adsorption.[17] Attempts at trapping this CF_4 were unsuccessful most likely because the gas is displaced from the bundle by either the ozone functionalization step or by the oxygen impurity present in the ozone gas stream. The displacement of physisorbed gases by other species is well-documented in the literature.[1,15,17,18] It should be no surprise that displacement is a potential complication in trapping more weakly bound gases. Reduction of the oxygen content of the ozone/oxygen stream could reduce displacement. Techniques for purifying ozone/oxygen mixtures have been reported in the literature,[36] and these could be effective in enhancing our trapping procedure.

Summary

A simple technique was described for trapping SF_6, CO_2, and $^{13}CO_2$ into single-walled carbon nanotube (SWNT) bundles. The procedure uses commercially available equipment and should be adaptable to most laboratories. The technique involves cryogenic adsorption of the gas into the SWNT bundle. The gas is then locked into its physisorption sites by functionalization with ozone. The trapped gases are stable in these bundles for periods of 24−72 h under vacuum. The trapped gases can be released by vacuum-heating to 700 K. The controlled trapping and release of gases clearly illustrate that SWNT bundles can be used as nanometer-sized gas storage and delivery systems for small quantities of gases.

Acknowledgment. Reference in this work to any specific commercial product is to facilitate understanding and does not necessarily imply endorsement by the United States Department of Energy.

References and Notes

(1) Byl, O.; Kondratyuk, P.; Yates, J. T. *J. Phys. Chem. B* **2003**, *107*, 4277.

(2) Radosavljevic, M.; Appenzeller, J.; Avouris, P.; Knoch, J. *Appl. Phys. Lett.* **2004**, *84*, 3693.
(3) Wei, J.; Zhu, H.; Wu, D.; Wei, B. *Appl. Phys. Lett.* **2004**, *84*, 4869.
(4) Novak, J.; Snow, E.; Houser, E.; Park, D.; Stepnowski, J.; McGil, R. *Appl. Phys. Lett.* **2003**, *83*, 4026.
(5) Lu, Y.; Han, J.; Ng, H.; Binder, C.; Partridge, C.; Meyyappan, M. *Chem. Phys. Lett.* **2004**, *391*, 344.
(6) Nguyen, C.; Delzeit, L.; Cassell, A.; Li, J.; Han, J.; Meyyappan, M. *Nano Lett.* **2002**, *2*, 1079.
(7) Gadd, G. E.; Blackford, M.; Moricca, S.; Webb, N.; Evans, P. J.; Smith, A. M.; Jacobsen, G.; Leung, S.; Day, A.; Hua, Q. *Science* **1997**, *277*, 933.
(8) Khlobystov, A.; Scipioni, R.; Nguyen-Manh, D.; Britz, D.; Pettifor, D.; Briggs, G. *Appl. Phys. Lett.* **2004**, *84*, 792.
(9) Khlobystov, A.; Britz, D.; Ardavan, A.; Briggs, G. *Phys. Rev. Lett.* **2004**, *92*, 245507.
(10) Gloter, A.; Suenaga, K.; Kataura, H.; Fujii, R.; Kodama, T.; Nishikawa, H.; Ikemoto, I.; Kikuchi, K.; Suzuki, S.; Achiba, Y.; Iijima, S. *Chem. Phys. Lett.* **2004**, *390*, 462.
(11) Takenobu, T.; Takano, T.; Shiraishi, M.; Murakami, Y.; Ata, M.; Kataura, H.; Achiba, Y.; Iwasa, Y. *Nat. Mater.* **2003**, *2*, 683.
(12) Matranga, C.; Bockrath, B. *J. Phys. Chem. B* **2004**, *108*, 6170.
(13) Matranga, C.; Chen, L.; Smith, M.; Bittner, E.; Johnson, J. K.; Bockrath, B. *J. Phys. Chem. B* **2003**, *107*, 12930.
(14) Chiang, I.; Brinson, B.; Huang, A.; Willis, P.; Bronikowski, M.; Margrave, J.; Smalley, R.; Hauge, R. *J. Phys. Chem. B* **2001**, *105*, 8297.
(15) Matranga, C.; Chen, L.; Bockrath, B.; Johnson, J. K. *Phys. Rev. B* **2004**, *70*, 165416.
(16) Herzberg, G. *Infrared and Raman Spectra*; D. Van Nostrand Company: Princeton, NJ, 1960; p 286.
(17) Byl, O.; Kondratyuk, P.; Forth, S.; Fitzgerald, S.; Yates, J. T. *J. Am. Chem. Soc.* **2003**, *125*, 5889.
(18) Yim, W.; Byl, O.; Yates, J. T.; Johnson, J. K. *J. Chem. Phys.* **2004**, *120*, 5377.
(19) Kuznetsova, A.; Mawhinney, D. B.; Naumenko, V.; Yates, J. T.; Liu, J.; Smalley, R. E. *Chem. Phys. Lett.* **2000**, *321*, 292.
(20) Mawhinney, D. B.; Naumenko, V.; Kuznetsova, A.; Yates, J. T. *J. Am. Chem. Soc.* **2000**, *122*, 2383.
(21) Itkis, M.; Niyogi, S.; Meng, M.; Hamon, M.; Hu, H.; Haddon, R. *Nano Lett.* **2002**, *2*, 155.
(22) Feng, X.; Matranga, C.; Vidic, R.; Borguet, E. *J. Phys. Chem. B* **2004**, *108*, 19949.
(23) Kuznetsova, A.; Popova, I.; Yates, J. T.; Bronikowski, M. J.; Huffman, C. B.; Liu, J.; Smalley, R. E.; Hwu, H. H.; Chen, J. G. *J. Am. Chem. Soc.* **2001**, *123*, 10699.
(24) Picozzi, S.; Santucci, S.; Lozzi, L.; Cantalini, C.; Barato, C.; Sberveglieri, C.; Armentano, I.; Kenny, J. M.; Valentini, L.; Delly, B. *J. Vac. Sci. Technol., A* **2004**, *22*, 1466.
(25) Picozzi, S.; Santucci, S.; Lozzi, L.; Valentini, L.; Delly, B. *J. Chem. Phys.* **2004**, *120*, 7147.
(26) Lu, X.; Zhang, L.; Xu, X.; Wang, N.; Zhang, Q. *J. Phys. Chem. B* **2002**, *106*, 2136.
(27) Rinsland, C.; Goldman, A.; Stephen, T.; Chiou, L.; Mahieu, E.; Zander, R. *J. Quant. Spectr. Rad. Transfer* **2003**, *78*, 41.
(28) Kuznetsova, A.; Yates, J. T.; Simonyan, V. V.; Johnson, J. K.; Huffman, C. B.; Smalley, R. E. *J. Chem. Phys.* **2001**, *115*, 6691.
(29) Kuznetsova, A.; Yates, J. T.; Liu, J.; Smalley, R. E. *J. Chem. Phys.* **2000**, *112*, 9590.
(30) Banerjee, S.; Wong, S. *Nano Lett.* **2004**, *4*, 1445.
(31) Banerjee, S.; Wong, S. *J. Phys. Chem. B* **2002**, *106*, 12144.
(32) Cai, L.; Bahr, J.; Yao, Y.; Tour, J. *Chem. Mater.* **2002**, *14*, 4235.
(33) Arab, M.; Picaud, F.; Devel, M.; Ramseyer, C.; Girardet, C. *Phys. Rev. B* **2004**, *69*, 165401.
(34) Stan, G.; Bojan, M. J.; Curtarolo, S.; Gatica, S. M.; Cole, M. W. *Phys. Rev. B* **2000**, *62*, 2173.
(35) Simonyan, V. V.; Johnson, J. K.; Kuznetsova, A.; Yates, J. T. *J. Chem. Phys.* **2001**, *114*, 4180.
(36) Zhukov, I.; Popova, I.; Yates, J. T. *J. Vac. Sci. Technol., B* **2000**, *18*, 992.